Proceedings of the 21st ICSMGE, Vienna, Austria, 14 – 19 June 2026. Pistrol, Adam & Schweiger (eds.)
Published by: ÖGG, Austrian Society for Geomechanics, Salzburg, Austria, ISBN 978-3-9503898-4-5
https://doi.org/10.53243/ICSMGE2026-413

Dynamic Modeling in the Frequency Domain: Horizontal Stiffness and Damping of a Square Footing on Sand Strata

Fardin Jafarzadeh
Department of Civil Engineering, Sharif University of Technology, Tehran, Iran, fardin@sharif.edu
The President of The Iranian Geotechnical Society, Tehran, Iran

Jafar Maleki
Geotechnical Engineer, Abgeer Consulting Engineers Company, Tehran, Iran
M.Sc. of Geotechnical Engineering, Sharif University of Technology, Tehran, Iran

ABSTRACT: This study examines the dynamic impedance functions of rigid square footings subjected to two-way horizontal harmonic loading, aiming to assess their frequency-dependent stiffness and damping characteristics. Experimental tests were conducted in a 1 m by 1 m by 0.8 m steel container filled with Babolsar sand, prepared at a 54% relative density using the sand raining method. Harmonic loads with controlled amplitude and frequency were applied using two shakers, with load cells and accelerometers measuring forces and displacements in horizontal and vertical directions. The results, presented as horizontal impedance functions versus dimensionless frequency, reveal that the presence of a rigid bedrock significantly influences wave propagation and energy dissipation, leading to increased stiffness and altered damping trends. Reducing the sand layer thickness from 55 cm to 40 cm slightly enhances dynamic stiffness at low frequencies, while footing mass has a negligible effect on impedance functions, supporting the massless foundation assumption. These findings highlight the critical role of soil layer geometry and boundary conditions in soil-foundation interaction, providing valuable data for the design of structures under dynamic loading.

KEYWORDS: Impedance function, physical modeling, horizontal loading, frequency domain, soil-foundation interaction.

1 INTRODUCTION

The dynamic response of shallow foundations under time-dependent loads is a critical aspect of soil-structure interaction, particularly for foundations subjected to harmonic and seismic excitations. A key components of modern dynamic analysis methods are the determination of impedance functions, which are defined as the ratios of applied interfacial forces or moments to the induced displacements or rotations of the foundation. These functions encapsulate the stiffness and damping characteristics of the soil-foundation system, which are influenced by factors such as soil type, loading frequency, and foundation geometry.

In recent years, a growing body of literature has explored numerical methods to predict the response of shallow foundations to dynamic loads, using models based on finite element methods, cone models, and mass-spring-damper systems (Pradhan et al., 2004; Seylabi et al., 2017). Large-scale experiments have provided valuable data for validating these numerical models, offering insights into real-world soil conditions (Dobry & Gazetas, 1986). However, small-scale physical modeling techniques offer better control over soil parameters, unlike in-situ testing, where the number of horizontal surfaces and boundary conditions are less manageable.

The dynamic behavior of shallow foundations is particularly complex in layered soil systems, where wave reflections from rigid boundaries significantly alter impedance functions compared to homogeneous half-space conditions. Recent advancements in experimental techniques, such as high-precision accelerometers and controlled harmonic loading systems, have enabled more accurate characterization of soil-foundation interactions under dynamic loads. Understanding the frequency-dependent response of square footings is crucial for optimizing the design of structures subjected to cyclic loading, such as wind turbines, industrial machinery, and seismic-resistant buildings. Furthermore, the influence of soil layer thickness and boundary conditions on impedance functions remains an area of active research, with implications for both theoretical models and practical engineering applications.

The dynamic response of shallow foundations in layered soil systems poses unique challenges due to the complex interplay of wave propagation, soil heterogeneity, and boundary conditions. Unlike homogeneous half-space assumptions commonly adopted in early studies, finite-thickness soil layers introduce wave reflections that significantly alter impedance functions, complicating the prediction of stiffness and damping characteristics. Recent research has highlighted the need for experimental data to validate numerical models, particularly for square footings, which are widely used in industrial and civil engineering applications. Previous studies, such as those by Nii (1987) and Dobry and Gazetas (1986), primarily focused on circular footings or vertical loading scenarios, leaving a gap in understanding the two-way horizontal response of square footings on layered soils. This study addresses these limitations by providing experimental insights into the frequency-dependent behavior of square footings, contributing to the development of more accurate design methodologies for dynamically loaded structures

Previous physical modeling studies have primarily focused on vertical or one-way horizontal loading scenarios. For instance, Nii (1987) investigated impedance functions for surface foundations under vertical vibrations in viscoelastic half-space conditions. Meanwhile, Jafarzadeh and Ghassemi (2011) explored one-way horizontal loading using physical models in half-space conditions, and Maleki and Jafarzadeh (2023) extended this research to rigid base conditions. Recently, Jafarzadeh and Maleki (2023 & 2025) further expanded this work to include two-way co-phase horizontal loading conditions for rigid circular footings.

This study addresses this gap by investigating the horizontal impedance functions of rigid square footings placed on a finite-thickness sand layer over a rigid base, subjected to two-way horizontal harmonic loading in the frequency domain. Using physical modeling in a controlled laboratory environment, the experiments utilize Babolsar sand prepared at a 54% relative density in a 1 m by 1 m by 0.8 m steel container. Harmonic loads are applied using a pair of shakers, and the responses are measured via load cells and accelerometers. The results, presented as impedance functions versus dimensionless

frequency, highlight the influence of the rigid base on wave propagation and energy dissipation, as well as the effects of footing mass and sand layer thickness on the dynamic behavior of the soil-foundation system (Maleki, 2015).

2 TEST SETUP

This study investigates the dynamic response of square footings on a homogeneous rigid base subjected to bidirectional, co-phase horizontal loading through physical modeling experiments (Maleki, 2015).

2.1 *Steel Container*

The soil medium was prepared in a 1 m × 1 m × 0.8 m steel container, with internal surfaces lined with a 0.1 m thick layer of sawdust to enhance damping. The sawdust used for lining the test container exhibited a poured density of 3.1 kN/m³, a consolidated density of 7.04 kN/m³, and a modulus of elasticity of 0.36 mPa (Stasiak et al., 2015). A 0.1 mm thick plastic layer encased a wooden frame around the container's perimeter to ensure separation. A 15 cm thick concrete slab was placed at the base to simulate bedrock conditions (Figure 1).

Figure 1. Steel box, wood frame and sawdust.

2.2 *Soil, Sand Raining Method and Footing*

Babolsar sand, sourced from the coastal region south of the Caspian Sea in Northern Iran, was used as the soil medium. This soil, according to the USCS standard, is classified as SP. Laboratory tests determined the following void ratios for the sand: maximum (e_{max}) of 0.775, minimum (e_{min}) of 0.547, and average (e_{ave}) of 0.510. The sand's minimum and maximum dry unit weights were 15.45 kN/m³ and 17.8 kN/m³, respectively, with a specific gravity (G_s) of 2.753. The particle size distribution is shown in Figure 2.

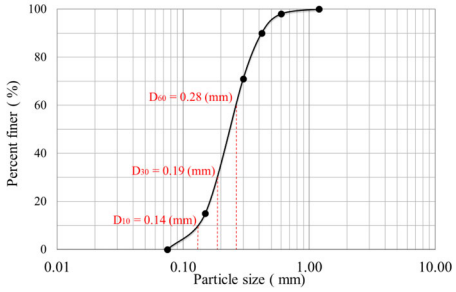

Figure 2. Particle size distribution for Babolsar sand.

To achieve uniform soil density, the sand was deposited using a sand-raining technique, where both the drop height and sand flux were controlled through a sieve with 6 mm openings. This air pluviation method involved releasing sand from a height of 70 cm, forming 5 cm thick layers with a relative density of approximately 54% (Figure 3). The soil was prepared in layers and resembled the condition of soil layers in nature. Through calibration tests, the relative unit weight of samples was adjusted. For the calibration test, cylindrical dishes were placed on the soil surface, and sand raining was done.

Figure 3. Sand Raining Method.

The experiments utilized square concrete footings with dimensions of 94 mm × 94 mm and a thickness of 50 mm, designed to prevent slipping during testing. The foundation was joined to a steel column with a height of 20 cm (Figure 4). In this research, the ratio of the steel container's length to the foundation equivalent diameter (800/106) was selected to reduce boundary effects on impedance functions, based on guidelines from Gazetas (1983).

Figure 4. a) the square footing, and b) the steel column.

2.3 *Signal generator, shaker, and instruments*

The experimental setup was designed to investigate the dynamic response of a soil-foundation system under co-phase horizontal harmonic loading. A steel column, 20 cm in height, was affixed to a footing placed at the center of the soil surface with zero embedment depth. The footing had a square shape and was placed centrally on the surface. A loading system, comprising of two shakers, metal rods, a harmonic signal generator, and a power amplifier, was integrated with the model. The shakers were supported by a steel adjustable frame. The signal generator could provide acceleration, velocity, and displacement over the frequency range of 1-10,000 Hz. The harmonic signal, generated by a signal analyzer and amplified, was transmitted through the metal rods to the column, applying horizontal loading to the footing. The metal rod was used to prevent excessive soil disturbance, and the load was applied to the footing in the horizontal directions. These rods were designed and made in a way that the axial to lateral stiffness ratio helped transfer as much load as possible in the axial direction.

The excitation frequency range was set between 50 and 900 Hz, covering the operational frequencies commonly found in industrial applications. The loading duration was 16 seconds and consisted of sinusoidal harmonic cycles at specific frequencies, with intervals of 20 Hz. Force amplitude was monitored using load cells positioned between the column and the metal rods, with voltage adjustments in the signal analyzer ensuring consistent horizontal loading across frequencies. Foundation displacements in both horizontal and vertical directions were measured using piezoelectric and strain-gauge accelerometers mounted on the footing. These sensors were connected to a data logger, which transmitted the data to a computer for analysis, enabling the calculation of the footing's

rotation angle. The schematic cross section of the model and the loading system are shown in Figure 5.

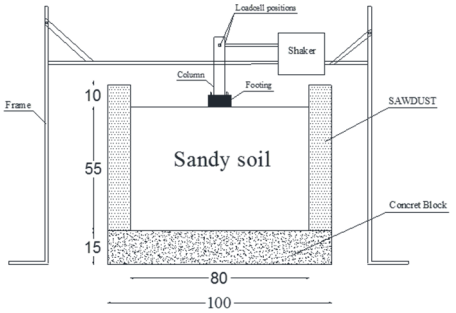

(a)

(b)

Figure 5. Physical model, (a) Schematic experimental setup (measurements are in centimeters), and (b) Real side view.

3 SUPPLEMENTARY TESTS

In order to investigate the dynamic properties of Babolsar sand models under rigid base conditions, travel time tests were carried out. Two accelerometers were placed 40 cm apart vertically within the soil model to determine pressure wave velocity. The accelerometers were then repositioned horizontally to measure shear wave velocity. A square footing was placed on top of the model, and vertical body waves were generated using a hammer. Several tests were conducted to ensure reliable results, with pressure and shear wave velocities determined to be 116 m/s and 54 m/s, respectively. The soil's dynamic properties were then calculated using classical elasticity theory, as summarized in Table 1.

Table 1. Dynamic Properties of Babolsar Sand Model

Parameter	Symbol	Value	Unit
Pressure wave velocity	V_p	116	m/s
Shear wave velocity	Vs	54	m/s
Shear modulus	G	4.8	mPa
Young's modulus	E	13.2	mPa
Poisson's ratio	υ	0.36	-
Relatively density	D_r	54	%
Dry density	γ_d	16.65	kN/m^3
Minimum dry density	$\gamma_{d,\,min}$	15.45	kN/m^3
Maximum dry density	$\gamma_{d,\,max}$	17.8	kN/m^3

Horizontal static stiffness (k_{sh}) was computed using Gazetas (1983), as Equation 1:

$$k_{sh} = \frac{8GR}{2-\upsilon}\left(1+\frac{R}{2H}\right) \quad (1)$$

where G is the shear modulus, ν is Poisson's ratio, H is the soil layer thickness, R is the equivalent footing radius, and H/R > 1. Tests for square footings with embedment ratios (D/h) of 0 and 1 yielded horizontal stiffness values of 1330 kN/m and 1324 kN/m, respectively. These dynamic properties provide essential data for analyzing soil-foundation interaction under rigid base conditions for square footings.

4 ANALYTICAL FRAMEWORK

The dynamic response of a soil-foundation system under horizontal vibrational loading is analyzed by modeling the interaction between the foundation and the supporting soil. Horizontal loading induces displacements and rotations in the soil, which are proportional to the applied vibration. Impedance functions, which relate the applied horizontal force at the soil-foundation interface to the resulting displacement or rotation, are frequency-dependent and are expressed in complex form as:

$$K_h = K_{1h}(\omega) + K_{2h}(\omega) = (k_h - m\omega^2) + (i\omega C_h) \quad (2)$$
$$= [k_{sh}.(k_h/k_{sh}) - m\omega^2] + i\omega.C_{sh}.(C_h/C_{sh})$$

in which both real component K_1 and imaginary component K_2 are functions of the circular frequency ω, m is the total mass of the foundation and machine, k_{sh} is the static horizontal stiffness and C_{sh} is the static damping coefficient, capturing damping due to energy dissipation through wave propagation (radiation damping) and material hysteresis, both frequency-dependent. The dimensionless frequency is calculated as:

$$a_0 = (\omega\, B)/(v_s) \quad (3)$$

where B is the half-width of the foundation, and V_s is the shear wave velocity of the soil. Results are presented as plots of k_h and C_h versus a_0, showing the variation of stiffness and damping with frequency.

To account for soil nonlinearity, an equivalent-linear approach is adopted. This method iteratively adjusts soil stiffness and damping based on the strain level induced by the horizontal load, improving the accuracy of impedance calculations under varying deformation conditions. For horizontal loading, the soil-foundation system experiences horizontal translation and rotation. Following Dunn (2010), coupled impedances are assumed to be negligible, and the horizontal impedance is calculated as:

$$K_h = \frac{F_S}{U_h} \quad (4)$$

where F_s is the effective horizontal force, and U_h is the maximum horizontal displacement at the soil-foundation interface. The force F_s accounts for the applied load and inertial effects, and is computed as:

$$F_S = F_T + \omega^2\,(M_0 U_b - M_0 b_2 \emptyset_b) \quad (5)$$

Here, F_T is the applied horizontal force, M_0 is the footing mass, U_b is the measured horizontal motion, b_2 is the distance from the instrumentation to the foundation's center of gravity, and ϕ_b is the maximum rotation angle. The horizontal displacement U_h and rotation ϕ_b are determined using:

$$U_h = U_b - 2b_2\varphi_b \quad (6)$$

$$\varphi_b = (v_1 + v_2)/2B \quad (7)$$

Where v_1 and v_2 are the maximum vertical displacements at opposite ends of the foundation base.

The data analysis procedure involves: (1) collecting data from load cells and accelerometers; (2) subtracting the mean from each dataset; (3) applying calibration coefficients to convert data into physical units; (4) filtering acceleration data

using a Band-Pass Filter (BPF) to isolate frequencies within a specified range, thereby mitigating unwanted frequencies; (5) integrating filtered acceleration data to obtain velocity and displacement; (6) transforming time-domain data into the frequency domain using Fourier series; and (7) computing impedance functions using the above equations. The BPF ensures that only frequencies relevant to the vibration are analyzed, thereby enhancing the accuracy of the frequency-domain results.

5 EXPERIMENTAL RESULTS

The experiments were performed with square footings under rigid base conditions, with the test program designed to minimize disturbances to the soil-foundation system. Key parameters, such as embedment ratio, footing inertia, and soil layer thickness, were selected to evaluate their impact on impedance functions. Additionally, it is important to recognize that factors like soil saturation, density, and construction-related disturbances can significantly influence horizontal impedance functions. Therefore, the mentioned and similar parameters should be accounted for when determining the impedance functions of soil-foundation systems.

As depicted in Figure 6, for square footings, the dynamic stiffness coefficient increases with a higher embedment ratio. The dynamic stiffness exhibited comparable trends at embedment ratios of 0 and 1. Additionally, fluctuations in dynamic stiffness were observed at dimensionless frequencies below 4.5. These variations may be attributed to the sharp edges of the square footing, which influence wave propagation within the soil medium. As the embedment ratio increases, the distance between the base of the square footing and the underlying rigid bed decreases, leading to enhanced wave reflection. This reflection amplifies the interaction between the foundation and the soil, significantly impacting the impedance results. Both experimental datasets indicate a peak in dynamic stiffness at $a_0 = 3.5$.

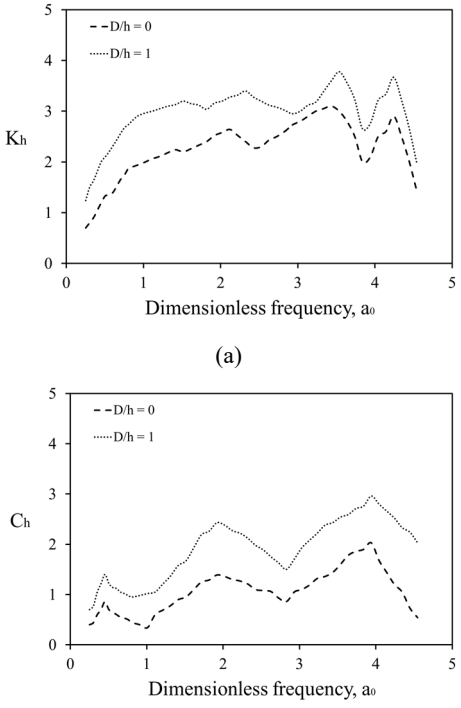

Figure 6. Comparison of the effect of embedded ratio on a) dynamic stiffness, and b) damping stiffness

Similarly, the dynamic damping coefficient in square footings rises with increasing embedment ratio, following consistent trends. The increase in both stiffness and damping with greater embedment can be explained scientifically by the enhanced soil confinement and contact area. A deeper embedment increases the lateral soil resistance and frictional interaction along the footing's sidewalls, contributing to higher stiffness. Additionally, the increased soil volume engaged in energy dissipation through wave radiation and hysteretic damping results in elevated damping coefficients. These effects are particularly pronounced in square footings due to their geometry, which promotes stronger soil-structure interaction compared to other shapes.

To investigate the influence of footing inertia on the dynamic response of a square footing, the mass of the foundation was increased from 2.4 kg to 3.5 kg by embedding four equal weights symmetrically on two opposite sides of the footing. As shown in Figure 7, this increase in footing mass had a negligible impact on the dynamic stiffness and damping coefficients of the soil-foundation system across the tested frequency range. These results suggest that the massless foundation theory (Gazetas, 1983), which assumes that the foundation's mass does not significantly affect dynamic stiffness and damping, remains largely valid for square footings.

The minimal influence of increased footing mass can be attributed to the dominant role of soil properties and geometry in governing the impedance functions. Dynamic stiffness and damping are primarily controlled by the soil's shear modulus, shear wave velocity, and the contact area between the footing and the soil, rather than the foundation's mass. For square footings, the relatively small increase in mass does not substantially alter the inertial effects compared to the soil's resistance to deformation and energy dissipation through wave radiation and hysteretic damping. Additionally, the symmetric placement of weights likely minimized any rotational inertia effects, further reducing the impact on the impedance functions.

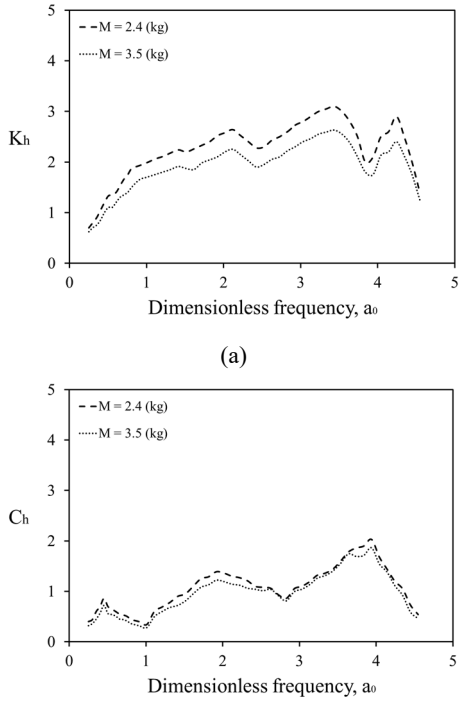

Figure 7. Comparison of the effect of the footing mass on a) dynamic stiffness. and b) damping stiffness

To evaluate the impact of soil layer thickness on the dynamic impedance functions of a square footing resting on sandy soil with a shear wave velocity of 54 m/s, the experimental setup was modified by adding a 15 cm thick layer of rigid concrete blocks to the model floor. This reduced the distance between the footing base and the top of the rigid bed from 55 cm to 40 cm. The experiments were repeated under these conditions, and the dynamic impedance functions were recalculated. As shown in Figure 8, reducing the soil layer thickness led to a slight increase in dynamic stiffness for the square footing at dimensionless frequencies below 4. For dynamic damping, the reduction in soil thickness had minimal impact at dimensionless frequencies less than 2, while at frequencies above 2, the damping exhibited an increasing but irregular trend.

The observed changes in impedance functions are primarily driven by the altered wave propagation dynamics in the thinner soil layer, influenced by the low shear wave velocity indicative of loose sandy soil. With a reduced soil layer thickness, stress waves experience increased reflections between the footing base and the rigid bed due to the shorter travel distance. These reflections enhance the soil's resistance to deformation, resulting in a modest increase in dynamic stiffness at lower frequencies. The limited effect at higher frequencies likely stems from the dominance of soil inertia and complex wave interactions, which reduce the influence of layer thickness. For damping, the negligible change at low frequencies suggests that energy dissipation through radiation and hysteretic damping is largely controlled by the soil's low shear modulus and limited capacity to propagate energy efficiently. At higher frequencies, the irregular increase in damping is attributed to intensified wave interference and scattering caused by the proximity of the rigid bed, which disrupts uniform energy dissipation. The low shear wave velocity results in longer wavelengths and slower wave propagation, amplifying these reflection effects in the thinner layer.

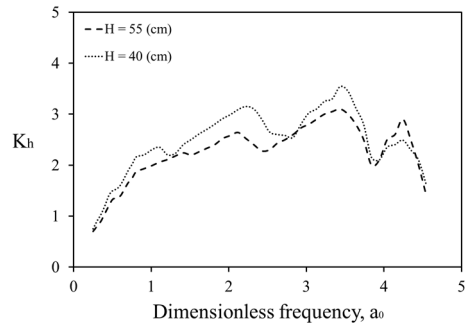

(a)

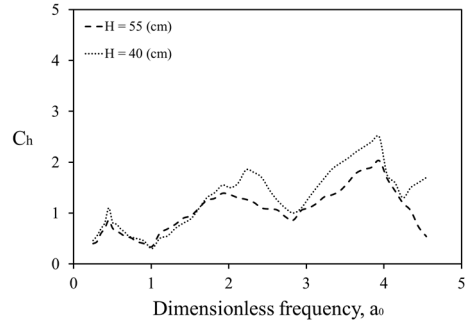

(b)

Figure 8. Comparison of the effect of the soil layer thickness on a) dynamic stiffness, and b) damping stiffness

The square footing's sharp edges further contribute to these responses by creating localized stress concentrations and complex wave patterns. In loose sandy soil with a low shear wave velocity, the soil's reduced ability to distribute stresses enhances the impact of these geometric effects, contributing to the observed stiffness fluctuations and irregular damping trends. These findings highlight the critical role of soil layer thickness and boundary conditions in shaping the dynamic response of soil-foundation systems under horizontal loading, particularly in soft soils where wave reflections dominate due to low wave speeds. The results emphasize the need to account for soil properties and layer geometry in the design of foundations subjected to dynamic loads.

The experimental results highlight the significant influence of soil layer thickness and boundary conditions on the dynamic impedance functions of square footings. Reducing the soil layer thickness from 55 cm to 40 cm increased dynamic stiffness by approximately 10% at dimensionless frequencies below 4, consistent with enhanced wave reflections from the rigid bedrock. In contrast, increasing the footing mass from 2.4 kg to 3.5 kg had a negligible effect on both stiffness and damping, supporting the massless foundation assumption for square footings. These findings align with Dobry and Gazetas (1986), who reported similar trends for circular footings, but extend their applicability to square geometries under two-way horizontal loading. The low shear wave velocity of models (54 m/s) amplified wave reflection effects, suggesting that soil stiffness and layer geometry dominate the dynamic response in loose soils. Limitations of the study include the small-scale nature of the experiments and the use of a single soil type, which may not fully represent field conditions. Future research should explore larger-scale tests and varied soil profiles to generalize these findings. These results provide critical insights for refining design guidelines for dynamically loaded foundations in layered soil systems.

6 APPLICATION OF EXPERIMENTAL RESULTS

To illustrate the practical application of the experimental impedance functions derived in this study, a realistic example is presented to calculate the horizontal displacement of a square footing supporting high-speed machinery under horizontal harmonic loading. The example is analogous to the dynamic stiffness and damping data obtained from physical model tests conducted in a 1 m × 1 m × 0.8 m steel container filled with Babolsar sand (shear wave velocity 54m/s and relative density of 54%).

Consider a square footing with a side length of 1 m (equivalent radius R = 0.564 m) resting on a 5.85 m thick sand layer above rigid bedrock. The soil thickness is scaled from the experimental setup (0.55 m) by a factor of approximately 10.64, maintaining geometric similarity between the model and prototype. The footing, constructed from reinforced concrete (density 2400 kg/m³), has a thickness of 0.5 m, resulting in a mass of approximately 1200 kg. The machine applies a harmonic horizontal force $F(t) = F_0 \sin(\omega t)$, with a force amplitude F_0 = 50 kN, typical for medium-sized industrial machinery such as compressors and pumps, and an excitation frequency f = 50 Hz (circular frequency $\omega = 2\pi f = 314$ rad/s), representative of high-speed equipment. The objective is to compute the maximum horizontal displacement, U_h.

The dimensionless frequency is calculated as $a_0 = \omega R/V_s = 314*0.564/54 \approx 3.28$. From the experimental impedance functions (Figure 6) at $a_0 \approx 3.28$, the dynamic stiffness ratio is approximately $k_h/k_{sh} \approx 2.95$, and the damping ratio is $C_h/C_{sh} \approx 1.28$, reflecting reduced stiffness and increased damping at higher frequencies.

The static horizontal stiffness k_{sh} is computed using Equation 1 (Gazetas, 1983), where $G = \rho.V_s^2 = (16.63*1000/9.81)*(54^2) = 4.94 * 10^6$ N/m^2, R = 0.564 m, υ = 0.36 and H = 5.85 m. This yields $k_{sh} \approx 2.526 * 10^7$ N/m. Thus, $k_h = 2.95 * 2.526 * 10^7 = 7.45 * 10^7$ N/m.

The static damping coefficient C_{sh} is estimated using Gazetas (1983):

$$C_{sh} = \frac{4GR^2}{V_S}\,\beta_h \tag{8}$$

Which $\beta_h = 0.75$ for loose sandy soil. So, by using Equation 8, the C_{sh} is calculated $8.73 * 10^4$ Ns/m. Given $C_h/C_{sh} \approx 1.28$ at $a_0 \approx 3.28$, C_h is $1.12 * 10^5$ Ns/m.

Considering a machine mass off approximately 1500 kg, the total mass of the foundation and machine will be about 2700 kg. The maximum horizontal displacement is calculated as:

$$U_h = \frac{F_0}{|K_h|} = \frac{F_0}{\sqrt{(k_h - m\omega^2)^2 + (\omega C_h)^2}} \tag{9}$$

That the U_h will find 0.261 mm. The calculated displacement is within acceptable limits for high-speed machinery per ACI 351.3R (2004), which recommends horizontal displacements below 0.2 mm for sensitive compressors but allows up to 0.8 mm for less critical equipment. The moderate displacement reflects significant energy dissipation due to wave reflections in the finite soil layer, consistent with the low shear wave velocity of loose sand. This low velocity amplifies wave reflections between the footing and the rigid bedrock, enhancing damping and reducing displacement compared to a half-space soil condition. To enhance design reliability, engineers could consider increasing soil compaction or adjusting footing dimensions to further reduce displacements. This example demonstrates the practical utility of the derived impedance functions for designing foundations subjected to dynamic loads, with clear scalability from laboratory to field conditions.

To further optimize the design, engineers could consider increasing soil compaction to enhance the shear modulus or adjusting the footing dimensions to reduce dynamic displacements. For instance, increasing the footing width or embedding it partially could further lower displacements, particularly for sensitive equipment.

7 CONCLUSION

This study provides valuable insights into the dynamic behavior of square footings on a finite-thickness sand layer under horizontal harmonic loading. The experimental results demonstrate that soil layer thickness and boundary conditions significantly influence the dynamic impedance functions, with a thinner soil layer leading to a slight increase in stiffness at low frequencies and irregular damping trends at higher frequencies. Conversely, footing mass has a negligible effect on impedance functions, supporting the applicability of massless foundation models for square footings in similar conditions.

The findings highlight the importance of considering soil properties, layer geometry, and boundary effects in the design of foundations subjected to dynamic loads. The verification example, using a 5.85 m soil layer scaled proportionally from the experimental setup and an excitation frequency of 50 Hz, illustrates the practical application of the derived impedance functions, predicting a displacement of 0.261 mm. These results contribute to the validation of physical modeling approaches and offer a foundation for refining numerical models used in soil-foundation-structure interaction analysis, particularly for structures on soft soils under high-frequency dynamic loading conditions.

The results underscore the importance of considering soil layer thickness and boundary conditions in the design of square footings subjected to dynamic loads. Engineers should prioritize soil compaction and layer geometry adjustments to mitigate excessive displacements in loose soils. Additionally, the experimental impedance functions can be integrated into numerical models, such as finite element simulations, to enhance the accuracy of dynamic response predictions. Future studies should investigate the effects of soil nonlinearity and multi-layered profiles to further refine these design methodologies.

8 REFERENCES

ACI Committee 351, 2004. Foundations for Dynamic Equipment (ACI 351.3R-04), American Concrete Institute, Farmington Hills, MI.

Dobry, R., and Gazetas, G. 1986. Dynamic response of arbitrarily shaped foundations. Journal of geotechnical engineering 112(2), 109-135.

Dunn, P. W. 2010. Comparison of cone model and measured dynamic impedance functions of shallow foundations. PhD Thesis, University of Florida.

Gazetas, G. 1983. Analysis of machine foundation vibrations: state of the art. International Journal of Soil Dynamics and Earthquake Engineering 2(1), 2-42.

Jafarzadeh, F., and Ghassemi, R. 2011. Investigation of Dynamic Response of Shallow Foundations to Horizontal Vibrations. In International Conference on Geotechnics for Sustainable Development (GEOTEC), Hanoi, Vietnam.

Jafarzadeh, F., and Maleki, J. 2023. Foundation impedance function from physical model tests by two-way horizontal loading. In Smart Geotechnics for Smart Societies, CRC Press, 1747-1753.

Jafarzadeh, F., and Maleki, J. 2025. Dynamic response of circular footing: Findings from experimental soil-foundation interactions. CRC Press.

Maleki, J. 2015. Horizontal Impedance Function of Surface Footings by Physical Model Tests. M.Sc. Thesis, Sharif University of Technology.

Maleki, J., and Jafarzadeh, F. 2023. Model tests on determining the effect of various geometrical aspects on horizontal impedance function of surface footings. Scientia Iranica.

Nii, Y. 1987. Experimental half-space dynamic stiffness. Journal of geotechnical engineering 113(11), 1359-1373.

Pradhan, P., Baidya, D., and Ghosh, D. 2004. Dynamic response of foundations resting on layered soil by cone model. Soil Dynamics and Earthquake Engineering. 24(6), 425-434.

Seylabi, E. E., Jeong, C., and Taciroglu, E. 2017. Modal and nodal impedance functions for truncated semi-infinite soil domains. Soil Dynamics and Earthquake Engineering, 92, 192-202.

Stasiak, M., Molenda, M., Bańda, M., and Gondek, E. 2015. Mechanical properties of sawdust and woodchips. Fuel. 159, 900-908.